

Antisolar differential rotation of slowly rotating cool stars

G. Rüdiger¹, M. Küker¹, P. J. Käpylä^{2,3}, and K.G. Strassmeier¹

¹ Leibniz-Institut für Astrophysik Potsdam (AIP), An der Sternwarte 16, D-14482 Potsdam, Germany, email: gruediger@aip.de

² Georg-August-Universität Göttingen, Institut für Astrophysik, Friedrich-Hund-Platz 1, D-37077 Göttingen, Germany

³ ReSoLVE Centre of Excellence, Department of Computer Science, Aalto University, PO Box 15400, FI-00076 Aalto, Finland

Received; accepted

ABSTRACT

It is well-known that rotating stellar convection transports angular momentum equatorward while a thermal energy flows poleward producing warm poles. The characteristic equatorial acceleration of the solar rotation law is a consequence of these phenomena. New numerical box simulations confirm the cross correlations $\langle u_r u_\theta \rangle$ and $\langle u_\theta u_\phi \rangle$ to be anticorrelated but their signs prove to be different for slow and fast rotation. The explanation is that for slow rotation large-scale circulation patterns appear which via viscosity terms change the signs of the cross correlations which transport angular momentum toward the poles and heat toward the equator. A so far neglected rotation-induced off-diagonal eddy viscosity term in connection with rotation laws with negative radial gradient, therefore, causes antisolar rotation laws with decelerated equator. The observation of decelerated equators at slowly rotating stars would thus lead to a better understanding of the active eddy viscosity tensor and the underlying turbulence.

Key words. convection – rotation – differential rotation – eddy viscosity

1. Introduction

Fast stellar rotation together with turbulent convection places its fingerprint on the stellar surface in form of starspots (Solanki 2003; Strassmeier 2009). There are still numerous puzzles for the quantitative description of the concerted action of stellar rotation and magnetic-field amplification in cool late-type stars. Differential surface rotation in its solar and antisolar form is one of them. Direct numerical and mean-field magnetohydrodynamic simulations deal with the impact of Reynolds stresses and thermal energy flows on angular momentum transport in rotating convection, which are thought to be responsible for the observed meridional flows and differential rotation, (e.g. Kitchatinov & Rüdiger 1999; Käpylä et al. 2011; Warnecke et al. 2013; Gastine et al. 2014; Featherstone & Miesch 2015). Kitchatinov & Olemskoy (2011) showed that the meridional flow is distributed over the entire convection zone in slow rotators but retreats to the convection zone boundaries in rapid rotators. Mean-field MHD simulations had already predicted antisolar differential rotation for stars with fast meridional circulation (Kitchatinov & Rüdiger 2004). Tracking sunspot and starspot migration from spatially resolved solar and stellar disk measurements (e.g. Künstler et al. 2015) provided us with direct observations of differential rotation also in its antisolar form (polar regions rotate faster than the equatorial regions) so that models can now be tested against observations.

Differential rotation from spot tracking is not confined to only solar observations anymore (for a summary of solar differential rotation tracing measurements see, e.g. Wöhl et al. 2010). Tracking starspot migration from spatially resolved stellar disk measurements (Doppler imaging) is a method to directly study stellar surface differential rotation. After pioneering work on image cross correlation and smeared Doppler imaging by Donati & Collier Cameron (1997), Barnes et al. (2005) concluded that differential rotation decreases with effective temper-

ature and rotation. We have now a number of (active) stars where differential rotation has been detected directly by means of Doppler imaging. A differential rotation versus rotation-period relationship from Doppler-imaging results was suggested by Kővári et al. (2017) in the form $\delta\Omega \simeq \pi/100$ rad/day, where $\delta\Omega$ is the equator-pole difference of the angular velocity. Such a very weak dependence of $\delta\Omega$ on the stellar rotation rate of dwarf stars and giants has first been predicted by Kitchatinov & Rüdiger (1999).

Space-based ultra-high precision time-series photometry allowed the confirmation of the temperature dependency of surface differential rotation for stars over a wide range in the HR-diagram (Reinhold et al. 2013). The observed $\delta\Omega$ only varied from 0.079 rad/day for cool stars ($T_{\text{eff}} = 3500$ K) to 0.096 rad/day for $T_{\text{eff}} = 6000$ K which is a rather weak variation of the observed differential rotation on the rotation periods. The hotter stars showing stronger differential rotation, peaking at the F stars where there is still a significant convective envelope but only comparably weak magnetic activity. On the contrary, the small differential rotation for M stars appears to be the most dynamo-efficient. The overall rate of rotation plays an observationally biasing role here because smaller stars rotate much faster than bigger stars. The comparison of the large set of differential rotation measures from the Kepler mission with the theoretical predictions by the Λ effect theory showed a fair agreement and gives us confidence in applying the method to a particular star. However, the photometric data does not contain information on the sign of differential rotation (but see Reinhold & Arlt (2015) for possible exceptions) and further spectroscopic time-series data are needed.

Benomar et al. (2018) report the asteroseismic detection of surface rotation laws of solar-type stars with rather large equator-pole differences of the angular velocity. Among the sample of 40 stars there are up to 10 candidates for antisolar differential rotation with a weak anticorrelation to rapid rotation.

In this paper we present numerical 3D simulations of rotating convection with a fixed Prandtl number. Our differential rotation model is described in Sect. 2. Simulations of rotating convection boxes are presented in Sect. 3. The results in terms of the eddy viscosity tensor for the angular momentum flow are given in Sect. 4 and discussed in Sect. 5.

2. Differential rotation

The symmetry properties of the cross correlations $Q_{r\phi}$ and $Q_{\theta\phi}$ differ from those of all other components of the one-point correlation tensor $Q_{ij} = \langle u_i(\mathbf{x}, t) u_j(\mathbf{x}, t) \rangle$ of a rotating turbulence field. The vector \mathbf{u} describes the fluctuating velocity in the turbulence field and later on \mathbf{U} will give the large-scale background velocity. While $Q_{r\phi}$ and $Q_{\theta\phi}$ are antisymmetric with respect to the transformation $\Omega \rightarrow -\Omega$, all other correlations are not. The turbulent angular momentum transport is thus odd in Ω while the other two tensor components – the cross correlation $Q_{r\theta}$ included – are even in Ω . It is easy to show that $Q_{r\phi}$ is symmetric with respect to the equator if the averaged flow is also symmetric. In this case the component $Q_{\theta\phi}$ is antisymmetric with respect to the equator. These rules can be violated if, for example, a magnetic field exists whose amplitudes are different in the two hemispheres.

One can also show that isotropic turbulence even under the influence of rotation does not lead to finite values of $Q_{r\phi}$ and $Q_{\theta\phi}$. With a preferred direction \mathbf{g} a tensor $(\epsilon_{ikl} g_j + \epsilon_{jkl} g_i) g_k \Omega_l$ linear in Ω exists which indeed possesses cross correlations with the index ϕ as one of the indices (if \mathbf{g} is radially directed). Rotating anisotropic turbulence, therefore, is able to transport angular momentum. The spherical coordinates (r, θ, ϕ) are used in this paper if the global system is concerned while (x, y, z) represent these coordinates in a Cartesian box geometry.

In the following the theory of differential rotation in shellular convection zones is briefly reviewed in the mean-field hydrodynamic approach. For the zonal fluxes of angular momentum we write

$$Q_{r\phi} = -\nu_T \sin \theta \frac{r \partial \Omega}{\partial r} + \hat{\nu}_T \Omega^2 \sin^2 \theta \cos \theta \frac{\partial \Omega}{\partial \theta} + \nu_T V \sin \theta \Omega \quad (1)$$

for the radial flux and

$$Q_{\theta\phi} = -\nu_T \sin \theta \frac{\partial \Omega}{\partial \theta} + \hat{\nu}_T \Omega^2 \sin^2 \theta \cos \theta \frac{r \partial \Omega}{\partial r} + \nu_T H \cos \theta \Omega \quad (2)$$

for the meridional flux. Here the first terms come from the Boussinesq diffusion approximation with ν_T as the positive standard eddy viscosity while V and H form the components of the Λ tensor describing the angular momentum transport of rigidly rotating anisotropic turbulence. The terms with $\hat{\nu}_T$ follow from the fact that a viscosity tensor connects the Reynolds stress with the deformation tensor¹. The non-diffusive terms in the zonal fluxes (1) and (2) can be written by means of the stress-strain tensor relation $Q_{i\phi} = -\mathcal{N}_{ij} \nabla_j \Omega$ with

$$\mathcal{N} = r \begin{pmatrix} \sin \theta \nu_T & -\cos \theta \sin^2 \theta \Omega^2 \hat{\nu}_T & 0 \\ -\cos \theta \sin^2 \theta \Omega^2 \hat{\nu}_T & \sin \theta \nu_T & 0 \\ 0 & 0 & 0 \end{pmatrix} \quad (3)$$

¹ $\hat{\nu}_T = \nu_2$ in the notation of Kitchatinov et al. (1994)

(Rüdiger 1989). The positive standard eddy viscosity ν_T is quenched by fast rotation. On the other hand, Kitchatinov et al. (1994) have shown that for isotropic and homogeneous turbulence $\hat{\nu}_T$ is positive for steeply decreasing frequency spectra. We shall call $\hat{\nu}_T$ as the rotation-induced off-diagonal viscosity term. At the poles *and* at the equator the off-diagonal viscosity does not contribute. Note that this term in Eq. (2) transforms a positive (negative) radial Ω gradient into positive (negative) cross correlations which – as the solution of the equation for the angular momentum conservation – finally leads to accelerated (decelerated) equators. Hence, the rotation law of a convection zone can never be only radius-dependent (Taylor-Proudman theorem). If the inner parts rotate faster than the outer parts (“sub-rotation”) then automatically the polar regions rotate (slightly) faster than the more equatorial regions and vice versa.

In accordance with earlier studies the following expansion is used for the normalized Λ effect:

$$V = \sum_{l=0} V^{(l)} \sin^{2l} \theta \sin \theta, \quad H = \sum_{l=1} H^{(l)} \sin^{2l} \theta \cos \theta. \quad (4)$$

The coefficients $V^{(l)}$ and $H^{(l)}$ describe the latitudinal profile of the Λ effect. Quasilinear theory of rapidly rotating anisotropic turbulent convection in the high-viscosity limit leads to $-V^{(0)} = V^{(1)} = H^{(1)} > 0$ (with $V^{(l)} = H^{(l)} = 0$ for $l > 1$) which implies that i) $Q_{r\phi}$ vanishes at the equator and ii) $-H \cos \theta$ is the angular momentum flow in axial direction. The function $H = H(\Omega)$ is positive definite so that the angular momentum is exclusively transported from pole to equator parallel to the rotation axis and $V^{(0)}$ is always negative.

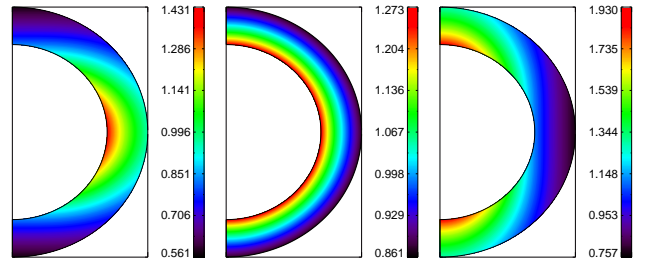


Fig. 1. Color-coded contours of the rotation law due to the Λ effect with $V^{(0)} = -1$, $V^{(1)} = 0$ and $H^{(1)} = 1$ (left), $H^{(1)} = 0$ (middle), $H^{(1)} = -1$ (right). Meridional circulation and the off-diagonal eddy viscosity are artificially suppressed. Positive $H^{(1)}$ lead to solar-type equatorial acceleration while negative $H^{(1)}$ lead to antisolar rotation profiles. $\hat{\nu}_T = 0$.

Either of the above-mentioned theories and simulations of the radial Λ effect lead to results of the form $V \propto -\cos^2 \theta$, i.e. $V^{(0)} < 0$ and $V = 0$ at the equator. For slow rotation $V^{(l)}$ and $H^{(l)}$ with $l > 0$ become so small that a radial rotation law with

$$\frac{d \log \Omega}{d \log r} = V^{(0)} \quad (5)$$

results. Negative $V^{(0)}$ generally lead to radial Ω profiles with negative shear. In this case a meridional circulation is driven by the centrifugal force which at the surface transports angular momentum towards the poles (“counterclockwise flow”). Hence, the equator rotates slower than the mid-latitudes so that an antisolar rotation law with $\cos \theta \partial \Omega / \partial \theta < 0$ (at the surface) automatically results.

Meridional flow and $\hat{\nu}_T$ neglected, the Reynolds stress (4) maintains a latitude-dependent surface rotation law $\Omega = \Omega(\theta)$ with

$$\frac{\delta\Omega}{\Omega} = -\frac{1}{2} \sum_{l=1} \left(d V^{(l)} + \frac{H^{(l)}}{l} \right) \quad (6)$$

for the pole-equator difference of Ω with the normalized thickness d of the convectively unstable layer with stress-free boundary conditions. Under the assumption that $V^{(l)} = H^{(l)} = 0$ for $l > 1$ antisolar rotation, therefore, would only be possible for (formally) negative $H^{(1)}$.

Figure 1 demonstrates the analytical expression (6). The equation of angular momentum is solved for a negative $V^{(0)}$. Meridional circulation and the off-diagonal viscosity $\hat{\nu}_T$ have been neglected. The latitudinal Λ effect denoted by $H^{(1)}$ is varied from 1 to -1 . Not surprisingly, a negative pole-equator difference of the surface rotation law (solar-type differential rotation) originates from $H^{(1)} = 1$ (left panel). For $H^{(1)} = -1$ the solar-type surface rotation law changes to an antisolar-type surface rotation law with positive pole-equator difference (right panel).

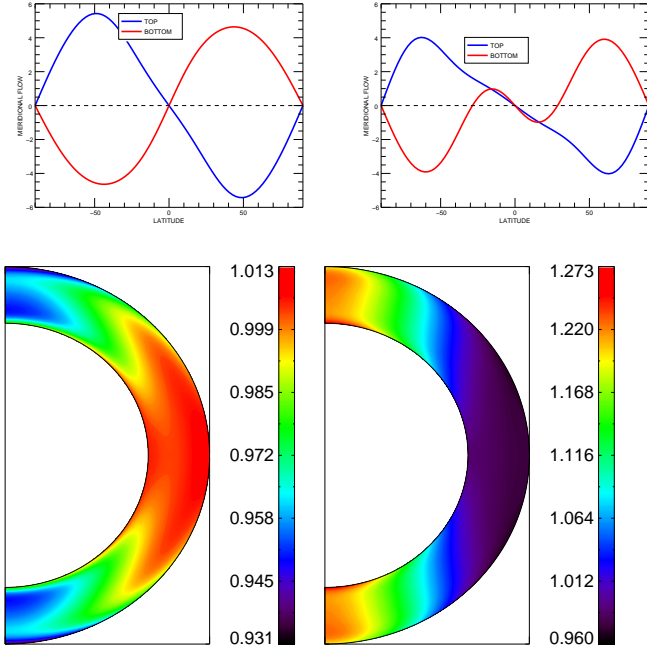


Fig. 2. Top: The meridional circulation (given as its Reynolds number) at top (blue) and bottom (red) of the convection zone associated with rotation laws shown in Fig. 1. Negative values at the surface of the northern hemisphere indicate a poleward directed circulation pattern (counterclockwise flow). There is always only one cell per hemisphere. Bottom: Similar to Fig. 1 but with meridional circulation included. Positive $H^{(1)}$ lead to solar-type acceleration of the equator (left panels). As a consequence of the (slow) counterclockwise meridional flow $H^{(1)} = 0$ leads to a weak antisolar-type equatorial deceleration (right panels).

Several analytical studies of the Λ effect led to positive $H^{(1)}$, i.e. $\cos\theta Q_{\theta\phi} > 0$, for rigid rotation. Also numerical simulations of rotating convection (Hupfer et al. 2006) or driven anisotropic turbulence under the influence of solid-body rotation (Käpylä

2019) provide equatorward transport of angular momentum. Earlier, Chan (2001) found equatorward transport only for fast rotation while for slow rotation occasionally the opposite result appeared. Simulations by Rüdiger et al. (2005) of rotating turbulent convection with much higher resolution provided very small $Q_{\theta\phi}$ for slow rotation and large positive $Q_{\theta\phi}$ for fast rotation. There seems to be no hope, therefore, to explain antisolar rotation laws for rotating stars with a hydrodynamical theory of turbulent rotating flows. In this paper numerical simulations of rotating convection in boxes are presented providing poleward transport of angular momentum for slow rotation. This poleward transport, however, does not result from the Λ effect but it is due to the rotation-induced off-diagonal viscosity term $\hat{\nu}_T$ in (2) in connection with a sub-rotation law ($\partial\Omega/\partial r < 0$) which appears for slow rotation. For solar-like convection zones with rotation profiles which are quasi-uniform in radius the $\hat{\nu}_T$ term will not play an important role.

The above finding that formally negative H easily produces antisolar rotation profiles remains true if also the meridional circulation as a consequence of radial shear is taken into account. The vorticity of the circulation depends on the sign of $\partial\Omega/\partial r$ (Kippenhahn 1963). At the surface it flows equatorward for super-rotation and poleward for sub-rotation. On the other hand, a circulation which flows equatorward at the surface of the convection zone (“clockwise flow”) produces differential rotation with an accelerated equator while it produces a polar vortex if it flows poleward (“counterclockwise flow”). One takes from Fig. 2 (top) that for all choices of $H^{(1)}$ the meridional circulation flows counterclockwise in the northern hemisphere so that it reduces the equatorial acceleration (left panel) or amplifies equatorial deceleration (right panel). Indeed, with circulation included, the left bottom plot of Fig. 2 with $H^{(1)} > 0$ represents a model for convection zones with solar-type rotation laws while the right panel of Fig. 2 with vanishing $H^{(1)}$ represents an antisolar rotation law.

3. Rotating convection

We perform simulations for convection with a fixed ordinary Prandtl number $\text{Pr} = \nu/\chi$ with χ the thermal diffusion coefficient. We perform simulations with fixed Prandtl numbers. For stellar material the heat-conductivity χ strongly exceeds the other diffusivities. The Roberts number $q = \chi/\eta = \text{Pm}/\text{Pr}$ is thus much larger than unity. Characteristic values are $q = \text{O}(10^4)$ for the bottom of the solar convection zone (Ossendrijver 2003). Close to the solar surface the Roberts number becomes much smaller. From numerical reasons we must work with the approximate surface value $q = 1$.

The simulations are done with the NIRVANA code by Ziegler (2002), which uses a conservative finite volume scheme in Cartesian coordinates. The length scale is defined by the depth of the convectively unstable layer. We assume an ideal, fully ionized gas kept at a fixed temperature at the bottom and cooled at the top of box. Periodic boundary conditions are formulated in the horizontal plane. The upper and lower boundaries are impenetrable and stress-free. The initial state is convectively unstable in a layer that occupies half of the box. Convection sets in if the Rayleigh number exceeds its critical value. In the dimensionless units the size of the simulation box is $2 \times 6 \times 6$ in the x , y , and z directions, respectively. The lower and upper boundaries of the unstably stratified layer are located at $x = 0.8$ and $x = 1.8$, respectively. The numerical resolution is $128 \times 384 \times 384$ grid points. The stratification of density, pressure, and temperature is

piecewise polytropic. The density varies by a factor 5 over the depth of the box, i.e. the density scale height is 1.2. More technical details such as the boundary conditions are described in Rüdiger et al. (2012).

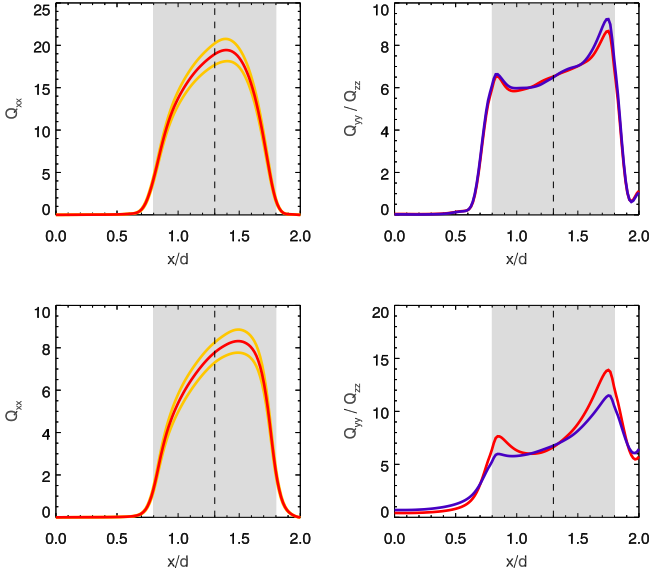


Fig. 3. Convection subject to very slow rotation ($\Omega = 1$, top) and to very fast rotation ($\Omega = 30$, bottom). Left: Q_{rr} , right: $Q_{\theta\theta}$ (red lines) and $Q_{\phi\phi}$ (blue lines). The shaded area indicates the convectively unstable part with the vertical dashed line showing its center, d is the depth of the convectively unstable layer. Correlations and rotation rate are given in code units. The volume-averaged turbulence intensity is $u_{\text{rms}}^2 = 28$, in code units. $\text{Pr} = 0.1$, $\theta = 45^\circ$.

Figure 3 gives the autocorrelations of the one-point correlation tensor Q_{ij} for convection subject to slow (top) and fast (bottom) rotation. The colatitude is $\theta = 45^\circ$. The Prandtl number is $\text{Pr} = 0.1$. The grey-shaded area is convectively unstable, its center is given by the vertical dashed line. As expected, the horizontal turbulent intensities are identical for slow rotation while the vertical intensity $\langle u_r^2 \rangle$ has the dominating value. It is suppressed, however, by faster rotation while the suppression of the horizontal components is much less. The radial turbulence intensity is reduced by more than a factor of two for $\Omega = 30$.

For driven turbulence in a quasilinear approximation we have

$$Q_{ij} = Q_{ij}^{(0)} - \varepsilon (2\Omega^2 \delta_{ij} - \Omega_i \Omega_j) \quad (7)$$

with

$$\begin{aligned} \varepsilon &= \frac{2}{15} \int_0^\infty \int_{-\infty}^\infty \frac{\nu^2 k^4 - 3\omega^2}{(\omega^2 + \nu^2 k^4)^2} E \, dk d\omega \\ &= -\frac{2}{15} \int_0^\infty \int_{-\infty}^\infty \frac{\omega}{(\omega^2 + \nu^2 k^4)^2} \frac{\partial}{\partial \omega} ((\omega^2 + \nu^2 k^4) E) \, dk d\omega \end{aligned} \quad (8)$$

(Rüdiger 1989). The sign of the expressions follows from the form of the positive-definite spectrum $E(k, \omega)$. It is obviously negative for white-noise spectra but it is positive for spectral functions which are sufficiently steep in ω . Also for the maximally steep spectrum such as $\delta(\omega)$ the ε is positive describing a rotational quenching of the turbulence intensities.

The vector of rotation at the colatitude θ is $\boldsymbol{\Omega} = \Omega(\cos \theta, -\sin \theta, 0)$ so that

$$\langle u_r^2 \rangle = \langle u_r^{(0)2} \rangle - \varepsilon \Omega^2 (2 - \cos^2 \theta) \quad (9)$$

results from Eq. (7). The rotational quenching of the radial turbulence intensity shown in Fig. 3 can be described by Eq. (9) with $\varepsilon > 0$.

Another direct consequence of (7) is the existence of the cross correlation of radial and latitudinal fluctuations, i.e.

$$Q_{r\theta} = -\varepsilon \Omega^2 \sin \theta \cos \theta, \quad (10)$$

which vanishes at poles and equator by definition. In a sense the correlation $Q_{r\theta}$ mimics the turbulent thermal conductivity tensor. If a radial temperature gradient exists a negative cross correlation $Q_{r\theta}$ organizes heat transport to the poles resulting in a meridional circulation towards the equator at the surface (Rüdiger et al. 2005).

For positive ε the rotation-induced cross correlation $Q_{r\theta}$ after (10) becomes negative. This theoretical result complies with the results of numerical simulations (Käpylä 2019). The expression (7) only describes the rotational influence on isotropic turbulence. Rüdiger et al. (2005) also considered the rotational influence on turbulence fields which are anisotropic in radial direction with the general result that always $Q_{r\theta} < 0$ (northern hemisphere) for steep spectra E and for all rotation rates.

From now on we shall switch to the Cartesian box coordinates x (representing the radial coordinate r), y (representing the colatitude θ) and z (representing the azimuth ϕ) hence $Q_{r\theta} \rightarrow Q_{xy}$, $Q_{r\phi} \rightarrow Q_{xz}$ and $Q_{\theta\phi} \rightarrow Q_{yz}$. The shears $r\partial\Omega/\partial r$ and $\partial\Omega/\partial\theta$ translate into dU_z/dx and dU_z/dy , resp. After averaging over the horizontal (yz) plane the relations (1) and (2) turn into

$$Q_{xz} = -\nu_T \frac{dU_z}{dx} + \nu_T V \sin \theta \Omega \quad (11)$$

and

$$Q_{yz} = \hat{\nu}_T \Omega^2 \cos \theta \sin \theta \frac{dU_z}{dx} + \nu_T H \cos \theta \Omega. \quad (12)$$

The cross correlation (10) completed by the viscosity term becomes

$$Q_{xy} = -\varepsilon \Omega^2 \sin \theta \cos \theta - \nu_T \frac{dU_y}{dx}. \quad (13)$$

The attention is here focused to the influence of the diffusion terms in Eqs. (12) and (13) in order to probe the existence of the viscosities ν_T and $\hat{\nu}_T$ by simulations. To this end the rotation rates are assumed so small that the non-diffusive terms in the relations (12) and (13) for the cross correlations are negligible. As an example, the second term in Eq. (13) is positive for (say) outwards decreasing meridional flow U_y . Then the cross correlation Q_{xy} should be positive for slow rotation and negative for rapid rotation changing the sign at a certain value of the parameter Ω (which denotes the angular velocity Ω of the rotation in code units). One finds such transition from positive to negative values for $5 < \Omega < 10$ in the simulations given in Fig. 4. The coincidence suggests that indeed the influence of viscosity terms in the expressions of cross correlations may lead to direction reversals of transport terms as function of rotation.

Without rotation all cross correlations vanish. For the slow-rotation models with $\Omega = 1$ already finite values appear (left plots in Figs. 4 and 5). At the radial boundaries the correlations Q_{xy} and Q_{xz} vanish by the boundary condition ($u_x = 0$) but

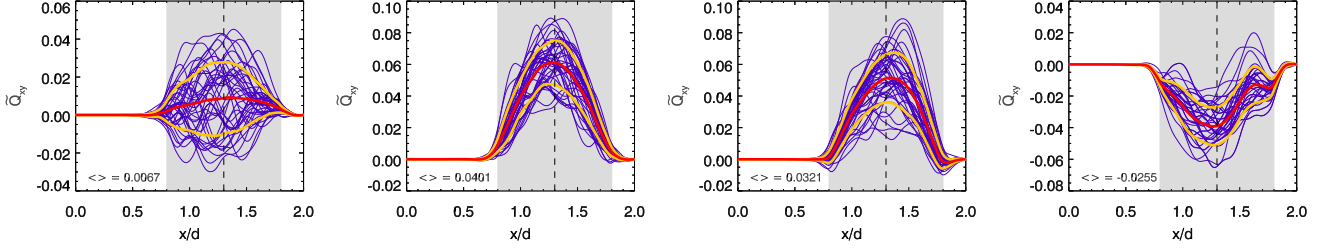


Fig. 4. Snapshots of the radial profiles of the radial cross correlation \tilde{Q}_{xy} (normalized with the volume-averaged rms velocity, u_{rms}^2) for $\Omega = 1$, $\Omega = 3$, $\Omega = 5$ and $\Omega = 10$ (from left to right). The sign changes for $\Omega > 5$ from positive to negative. The convectively unstable part of the box is grey-shaded. $\text{Pr} = 0.1$, $\theta = 45^\circ$.

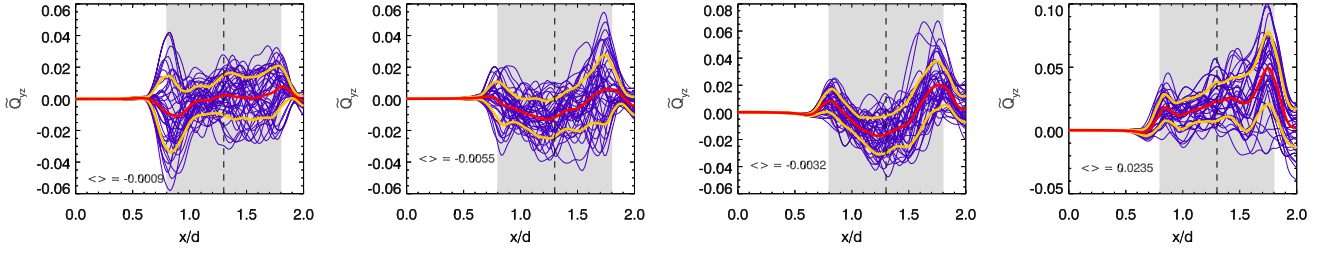


Fig. 5. Similar to Fig. 4 but for the horizontal cross correlation \tilde{Q}_{yz} . The sign changes for $\Omega > 5$ from negative to positive.

the horizontal cross correlation Q_{yz} remains finite. It is always positive at top and bottom of the unstable box which indicates $H > 0$ if a possible mean circulation U_z would be maximal or minimal at the top or bottom of the convection box (as it is, see Fig. 6).

The correlation Q_{xy} for slow rotation is positive so that heat is transported toward the equator. At the same time the horizontal correlation Q_{yz} presumes negative values. Independent of the rotation rates and for both hemispheres we find the general result that always $Q_{xy}Q_{yz} < 0$. The simulations show, therefore, that angular momentum flux to the equator (poles) is always accompanied by heat transport to the poles (equator). Somewhere between $\Omega = 5$ and $\Omega = 10$ the cross correlations Q_{xy} and Q_{yz} change their signs becoming negative (Q_{xy}) and positive (Q_{yz}) for fast rotation. These signs are well-known from the analytical expressions derived for driven turbulence for fast rotation. In this case the angular momentum is transported inward as well as toward the equator by the convection, or with other words, it flows along cylindrical surfaces.

For increasingly fast rotation the amplitudes of the negative Q_{xy} are increasing, contrary to Q_{yz} which sink. This is a basic difference for the two cross correlations. Note that for the transformation $\Omega \rightarrow -\Omega$ the correlations Q_{yz} change their sign which is not the case for Q_{xy} . The reason is that Q_{xy} is even in the rotational rate Ω while the horizontal cross correlation Q_{yz} is odd.

4. The eddy viscosities

Equation (10) neglects the influence of a possible radial shear dU_y/dx of a meridional flow. The question is whether large-scale mean flow characterizes the simulation box as in the simulations of Chan (2001) and Käpylä et al. (2004), which could be used to calculate the eddy viscosities after relations (12) and (13). The mean flows in the box have been calculated for slow

rotation. The top panel of Fig. 6 gives flows in meridional direction and the bottom panel gives zonal flows in azimuthal direction. The basic rotation there has been varied from $\Omega = 1$ to $\Omega = 10$ and the Prandtl number is fixed at $\text{Pr} = 0.1$. The following estimate concerns the first example with $\Omega = 1$ with the cross correlation $Q_{xy} \simeq 0.01u_{\text{rms}}^2$ (from Fig. 5) and the shear $\delta U_y/\delta x \simeq -0.2$ (from Fig. 6). The standard eddy viscosity ν_T in code units results to 1.5 for slow rotation. The microscopic viscosity of the model in the same units is $\nu = 6 \cdot 10^{-3}$ so that for the Reynolds number $\nu_T/\nu \simeq 240$. One finds very similar values for $\Omega = 3$.

The dimensionless eddy viscosity α_{vis} after

$$\nu_T = \alpha_{\text{vis}} \tau_{\text{corr}} u_{\text{rms}}^2. \quad (14)$$

may also be introduced which is often assumed in turbulence research as $\alpha_{\text{vis}} \simeq 0.3$. To find the correlation time τ_{corr} an auto-correlation analysis as done by Küker & Rüdiger (2018) is necessary. The result is $\tau_{\text{corr}} \simeq 0.1$ in code units, hence $\alpha_{\text{vis}} \lesssim 0.5$ which indeed is of the expected order of magnitude.

Figure 6 also demonstrates that the negative shear dU_y/dx is always accompanied by a negative shear dU_z/dx of the zonal flow, hence $dU_y/dx \cdot dU_z/dx > 0$. Transformed to the global system it means that a sub-rotating shell generates a counter-clockwise circulation where the fluid drifts poleward at the surface. This type of flow pattern has already been described in the text below Eq. (5). On the other hand, the existence of U_z allows to estimate the off-diagonal viscosity after Eq. (12) with $H \approx 0$ for $\Omega = 1$ or $\Omega = 3$ to $\hat{\nu}_T \simeq 0.05$, hence $\hat{\nu}_T/\nu_T \simeq 0.03$ in code units or $\hat{\nu}_T/\nu_T \simeq 3\tau_{\text{corr}}^2$ in physical units.

After Eqs. (11) and (12) the shear dU_z/dx contributes to the cross correlations Q_{xz} and Q_{yz} . Because of its negativity the viscosity term in (11) is positive so that the actual value of $|V|$ is even larger than indicated by Q_{xz} from the simulations.

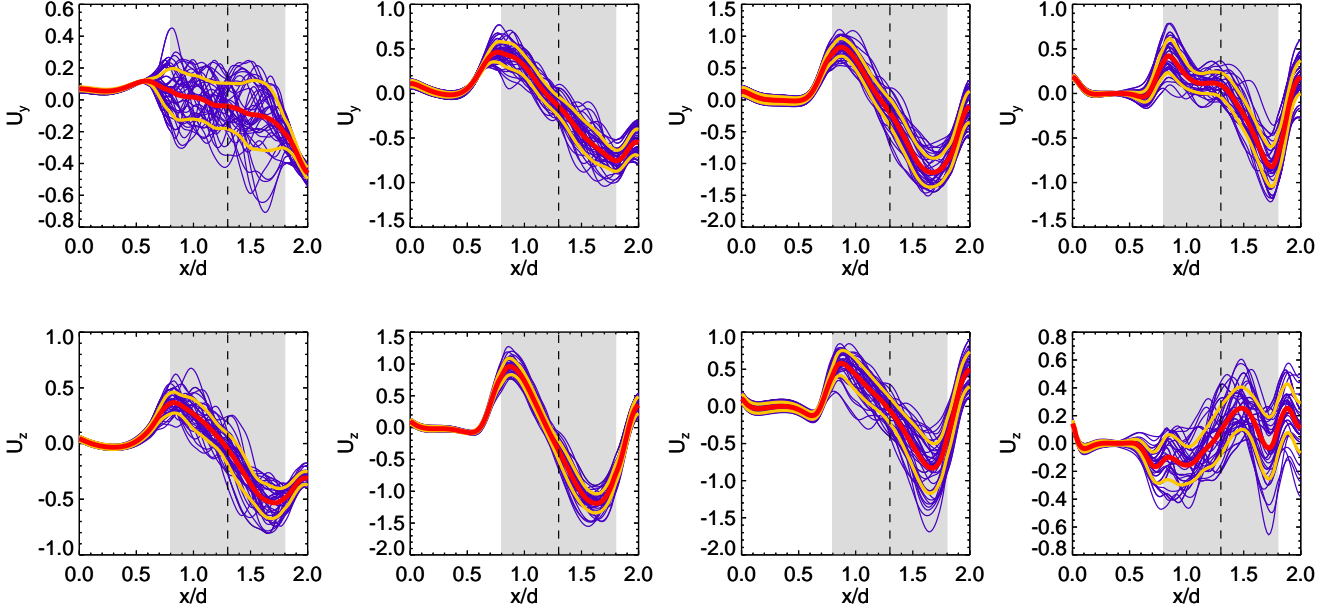


Fig. 6. Radial profiles of the meridional flow U_y (top) and zonal flow U_z (bottom) in the convective box (shaded). The parameters are $\Omega = 1$, $\Omega = 3$, $\Omega = 5$ and $\Omega = 10$ (from left to right). $\text{Pr} = 0.1$. The circulation is always counterclockwise and the rotation is decelerated at the surface (sub-rotation). $\theta = 45^\circ$.

4.1. Rotation-induced off-diagonal eddy viscosity

The same radial velocity gradient appears in the expression for the horizontal cross correlation in a higher order of the rotation rate. The two viscosities in (12) can be expressed by the integrals

$$\nu_T = \frac{2}{15} \int_0^\infty \int_{-\infty}^\infty \frac{\nu^3 k^6}{(\omega^2 + \nu^2 k^4)^2} E \, dk d\omega \quad (15)$$

and

$$\hat{\nu}_T = \frac{48}{105} \int_0^\infty \int_{-\infty}^\infty \frac{\nu k^2 \omega^2 (5\nu^2 k^4 - 3\omega^2)}{(\omega^2 + \nu^2 k^4)^4} E \, dk d\omega \quad (16)$$

(Rüdiger 1989). Not surprisingly, the first integral is positive definite. On the other hand, the second integral is positive for all other monotonously decreasing spectra because of

$$\hat{\nu}_T = \frac{48}{105} \int_0^\infty \int_{-\infty}^\infty \frac{\nu k^2 \omega^2}{(\omega^2 + \nu^2 k^4)^2} \left(\frac{E}{\omega^2 + \nu^2 k^4} - 2 \frac{\partial}{\partial \omega} \frac{\omega E}{\omega^2 + \nu^2 k^4} \right) dk d\omega. \quad (17)$$

It is even positive for spectra of the white-noise-type. For a demonstration the frequency integral in (16) is evaluated with uniform E . As

$$\int_{-\infty}^\infty \frac{\nu^3 k^6 \omega^2 (5\nu^2 k^4 - 3\omega^2)}{(\omega^2 + \nu^2 k^4)^4} d\omega = \frac{\pi}{8} \quad (18)$$

also here the $\hat{\nu}_T$ is positive. Note, however, that very steep spectra such as $\delta(\omega)$ lead to vanishing $\hat{\nu}_T$ which explains the absence of antisolar rotation laws in the calculations based on that turbulence model (Kitchatinov et al. 1994). It seems thus likely that observations of slowly rotating stars with decelerated equator questions the application of turbulences with δ -like frequency spectra in stellar convection modellings.

As the corresponding integral for the standard eddy viscosity (15) is $\pi/2$ one obtains for rather flat spectra $\hat{\nu}_T/\nu_T \simeq$

$(l_{\text{corr}}^2/2\nu)^2 \simeq \tau_{\text{corr}}^2$. The latter relation requires that for the background viscosity ν the standard expression $\nu \simeq 0.5 l_{\text{corr}}^2/\tau_{\text{corr}}$ is used. Because of $\hat{\nu}_T > 0$ and $dU_z/dx < 0$ (see Fig. 6) *negative* contributions to the horizontal cross correlation are produced. The existence of the off-diagonal viscosity $\hat{\nu}_T$, therefore, explains the resulting negativity of the cross correlation Q_{yz} for slow rotation (see Fig. 5). The result confirms the above finding that all values of Q_{yz} are positive at the top and bottom boundaries where the mean shear vanishes. For faster rotation the increasing positive values of H overcompensate the negative contribution from the radial shear of U_z which becomes increasingly unimportant (see Fig. 6). For the Sun as a rapid rotator (from our point of view) Hathaway et al. (2013) indeed report $\cos \theta Q_{\theta\phi} > 0$. The transition from negative to positive Q_{yz} happens in Fig. 5 for $\Omega \simeq 5$. Figure 6 also demonstrates that the shear dU_z/dx grows for $\Omega < 5$ and overcompensates the positive H term producing the obtained negative cross correlations.

As the mechanisms of the null crossings of Q_{xy} and Q_{yz} are different, the values for the critical Ω should not be identical for both cases.

4.2. Antisolar rotation

Models are considered of so slow rotation that $H \simeq 0$ and a (negative) $V^{(0)}$ exists besides the rotation-induced off-diagonal viscosity $\hat{\nu}_T$. The existence of the latter has been indicated by the simulations for the horizontal cross correlation Q_{yz} shown in Fig. 5. This leads to functions of H that are formally negative (for slow rotation) for which the Fig. 1 demonstrates the appearance of antisolar rotation laws. The off-diagonal element $\hat{\nu}_T$ is varied in Fig. 7 from $\hat{\nu}_T = -0.5$ (left panel) to zero (middle panel) and $\hat{\nu}_T = 0.5$ (right panel). For the models shown in the top row of the plots the resulting meridional circulation is artificially suppressed. One finds that negative $V^{(0)}$ always produces rotation laws with negative radial shear which in connection with positive $\hat{\nu}_T$ leads to antisolar rotation and vice versa.

Hence, for $V^{(0)}\hat{\nu}_T < 0$ the equator rotates slower than the polar regions and just this condition is the result of the given numerical simulations. One could also demonstrate that the equator is accelerated for $V^{(0)}\hat{\nu}_T > 0$ (not shown).

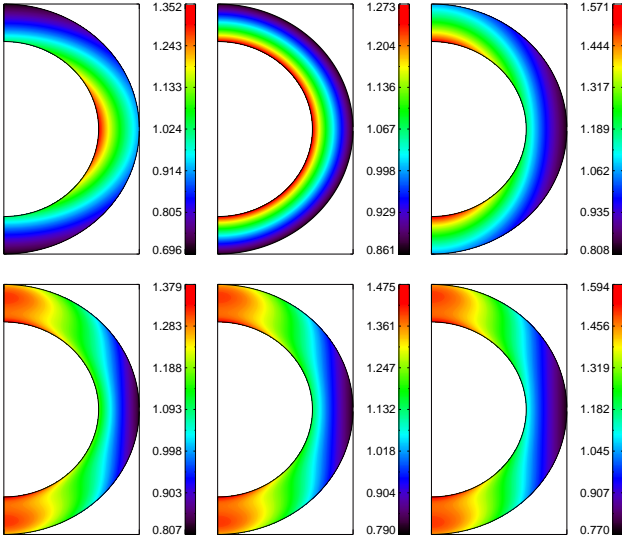


Fig. 7. Similar to Fig. 1 but for slow rotation ($V^{(0)} = -1$ and $V^{(1)} = H^{(1)} = 0$). The off-diagonal viscosity term varies from $\hat{\nu}_T = -0.5$ (left), $\hat{\nu}_T = 0$ (middle) to $\hat{\nu}_T = 0.5$ (right). Meridional circulation is suppressed (top) and it is included as in Fig. 2 (bottom). For positive $\hat{\nu}_T$ the rotation is always antisolar without and with meridional circulation. The circulation is always counterclockwise. Note the negative radial shear below the equator in all cases.

If, as done in the models in the second row of Fig. 7, also the associated meridional flow is allowed to transport angular momentum, the Ω isolines become cylindrical in accordance to the Taylor-Proudman theorem and the antisolar rotation law is only modified but not destroyed. Note, how in the middle panels (only) the meridional circulation changes the type of the rotation law from uniform on spherical shells to cylindric with respect to the rotation axis. The circulation cells always flow counterclockwise, i.e. poleward at the surface.

From the comparison of Figs. 1 and 7 one finds that antisolar rotation profiles result both for positive $\hat{\nu}_T$ in common with subrotation and/or for negative $H^{(1)}$. The latter can be excluded with numerical experiments where the U_y and U_z are artificially suppressed mimicking the existence of strict solid-body rotation. This has been confirmed by PENCIL CODE² simulations which use the same setup as in Käpylä (2018); see Fig. 8

Here we present results from a slowly rotating run with and without mean flows. The used Coriolis number $\text{Co} = \Omega d / \pi u_{\text{rms}} \approx 0.25$ corresponds to $\Omega \simeq 4$ in NIRVANA code units. We find that the signs of Q_{xy} and Q_{yz} change when the mean flows are suppressed. This is consistent with a dominating contribution from turbulent viscosity in Q_{xy} and the rotation-induced off-diagonal viscosity term in Q_{yz} in accordance with theory. Finally, we note that the magnitude of Q_{xz} also increases

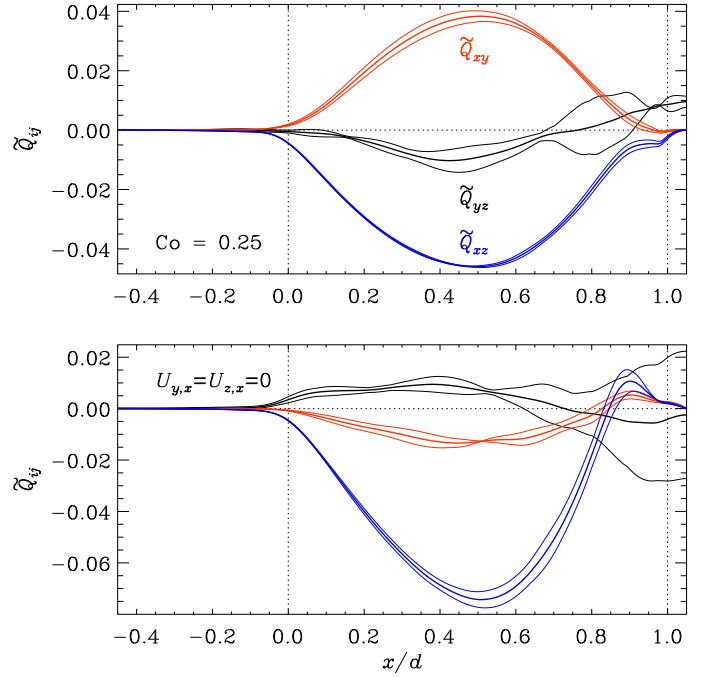


Fig. 8. Normalized off-diagonal Reynolds stresses as indicated by the legends from runs with (upper panel) and without (below) horizontal mean flows. The vertical dotted lines indicate top and bottom of the convection zone.

clearly in the case where the shear is suppressed, indicating a strong contribution from the term involving ν_T .

5. Discussion

The cross correlations $Q_{r\theta}$, $Q_{r\phi}$ and $Q_{\theta\phi}$ of the fluctuating velocities in a rotating turbulence are playing basic roles in understanding the rotation laws of stars with outer convection zones. Shortly speaking, the tensor component $Q_{r\theta}$ transports thermal energy in latitudinal direction (‘warm poles’) while $Q_{r\phi}$ and $Q_{\theta\phi}$ transport angular momentum in radial and meridional directions. For driven turbulence of a uniformly rotating density-stratified medium (stratified in radial direction) the correlations fulfill simple sign rules independent of the rotation rate: it is $Q_{r\theta} < 0$, $Q_{r\phi} < 0$ and $Q_{\theta\phi} > 0$, taken always in the northern hemisphere. In physical quantities it means that thermal energy is transported to the poles while the angular momentum is transported inward and equatorward. The resulting warm poles drive a clockwise meridional circulation (northern hemisphere) which together with the positive $Q_{\theta\phi}$ transports angular momentum towards the equator. Hence, if the convection zone can be modeled by driven turbulence under fast global rotation then the resulting surface rotation law will always be of the solar-type. The simultaneous solution of the Reynolds equation and the corresponding energy equation provides rotation profiles, meridional circulation patterns and pole-equator temperature differences which are rather close to observations (Kitchatinov & Rüdiger 1999; Küker et al. 2011). The results are similar for all rotation rates and the number of tuning parameters is only low.

There are, however, increasing observational indications for the existence of antisolar rotation laws where the equator rotates slower than the polar regions. The results of observations (Metcalf et al. 2016) as well as of numeri-

² <http://github.com/pencil-code>

cal simulations (Gastine et al. 2014) suggest stars with slow rotation as possessing antisolar rotation laws. Furthermore, Brandenburg & Giampapa (2018) argue in favor of the appearance of antisolar rotation laws for slow-rotators with large Rossby number.

We assume that because of the often stated positivity of the function H the horizontal Λ effect always transports angular momentum equatorward in favor of an accelerated equator. If, however, a rotation law with a negative radial gradient exists then the rotation-induced off-diagonal components of the eddy viscosity tensor such as $\hat{\nu}_T$ transport angular momentum poleward in favor of a polar vortex (“antisolar”). This also implies that a strictly radius-dependent rotation law $\Omega = \Omega(r)$ can never exist in (slowly) rotating convection zones. After the Taylor-Proudman theorem the rotation will tend to produce z -independent rotation laws hence a negative radial shear of the angular velocity is *always* accompanied by slightly accelerated polar regions.

We compute the cross correlations $Q_{r\theta}$, $Q_{r\phi}$ and $Q_{\theta\phi}$ from numerical simulations of convection in a rotating box. The averaging process concerns the horizontal planes so that only radial shear can influence the cross correlations (see Eqs. (1), (2) and (13)). For fast rotation the well-known findings of positive $Q_{\theta\phi}$ and negative $Q_{r\theta}$, $Q_{r\phi}$ are reproduced (northern hemisphere). For slow rotation, however, the signs of both $Q_{r\theta}$ and $Q_{\theta\phi}$ change almost simultaneously so that the angular momentum is now transported to the poles and the heat is transported to the equator. The resulting warm equator leads to a counter-clockwise meridional circulation which transports the angular momentum to the poles. The new signs of the quantities $Q_{r\theta}$ and $Q_{\theta\phi}$ may thus lead to antisolar differential rotation.

This behavior, however, is due to the appearance of large-scale flows in zonal and in meridional directions. The zonal flow U_z mimics a differential rotation with negative radial gradient. Via the off-diagonal viscosity in Eq. (2) (for positive $\hat{\nu}_T$) a negative contribution to $Q_{\theta\phi}$ results overcompensating the positive but small values of H . A similar effect happens for $Q_{r\theta}$ where the negative radial gradient of U_y in connection with the positive eddy viscosity ν_T provides positive contributions to the negative cross correlation (10). From the associated numerical values with Eq. (14) also ν_T can be calculated leading to $\nu_T/\nu \simeq 240$, or to the (reasonable) dimensionless quantity $\alpha_{\text{vis}} \lesssim 0.5$. The simulations lead to the relation $\hat{\nu}_T/\nu_T \simeq 3\tau_{\text{corr}}^2$ for the ratio of the rotation-induced off-diagonal viscosity term and the standard (diagonal) eddy viscosity.

We also probed the influence of the radial shears of the large-scale flows U_y and U_z on the cross correlations Q_{xy} and Q_{yz} with numerical experiments where the U_y and U_z can artificially be suppressed. In these cases for all rotation rates negative Q_{xy} and positive Q_{yz} resulted. Without large-scale flows the analytical results are confirmed that $Q_{r\theta} < 0$ and $Q_{\theta\phi} > 0$ for the northern hemisphere formulated in spherical coordinates. For slow rotation both signs are changed if the large-scale shear flows are allowed to back-react.

In summary, we have shown that a so far neglected rotation-induced off-diagonal eddy viscosity term (if large enough) in connection with rotation laws with negative radial gradient (sub-rotation, as existing in slowly rotating stars) is able to produce differential rotation of the antisolar-type. If indeed new observations confirm the existence of decelerated equators at slowly rotating stars then we shall better understand the nature of the active eddy viscosity tensor and the underlying turbulence model.

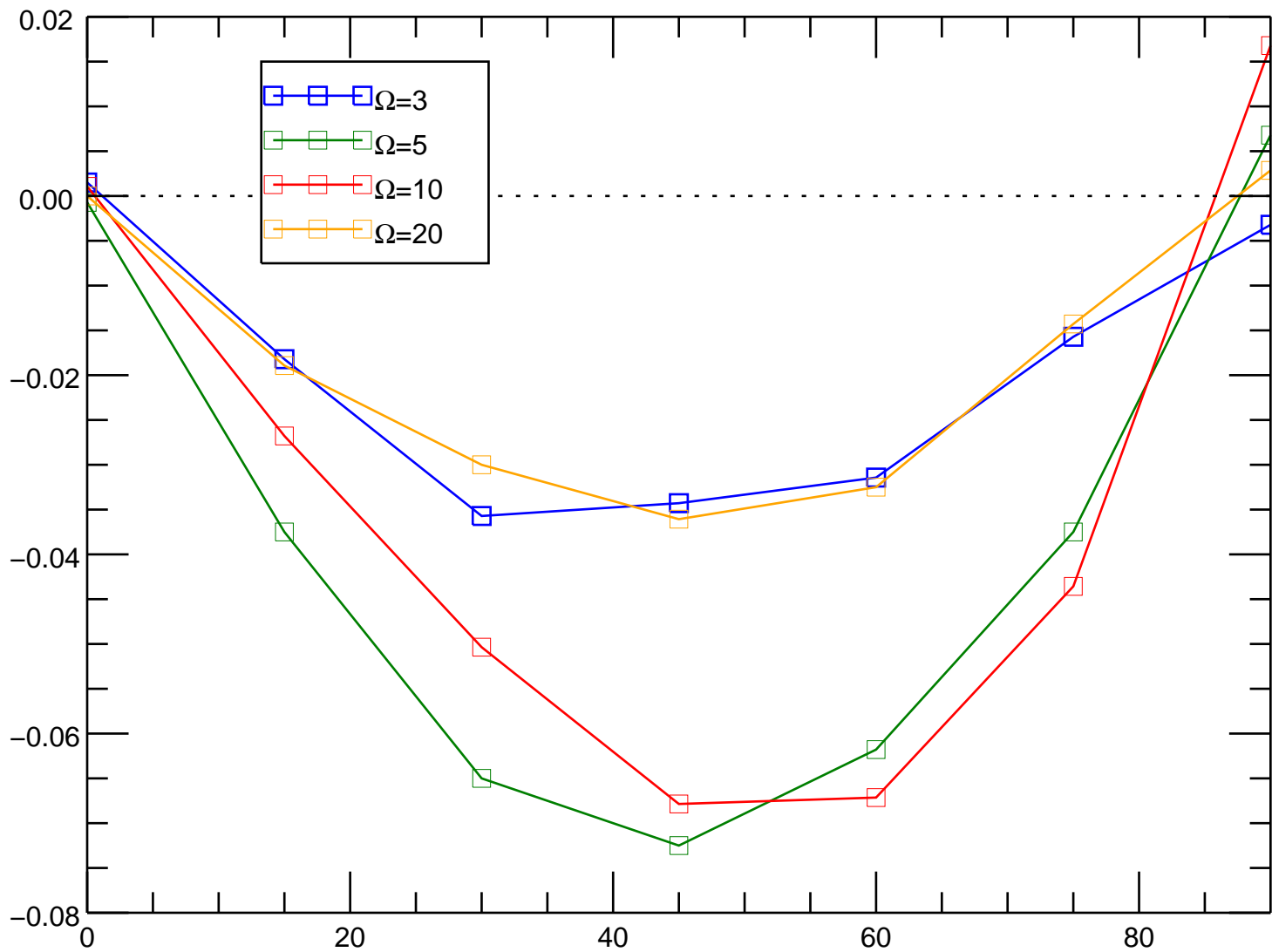
Acknowledgements. PJK acknowledges the computing resources provided by CSC – IT Center for Science, who are administered by the Finnish Ministry of Education; of Espoo, Finland, and the Gauss Center for Supercomputing

for the Large-Scale computing project “Cracking the Convective Conundrum” in the Leibniz Supercomputing Centre’s SuperMUC supercomputer in Garching, Germany. This work was supported in part by the Deutsche Forschungsgemeinschaft Heisenberg programme (grant No. KA 4825/1-1; PJK) and the Academy of Finland ReSoLVE Centre of Excellence (grant No. 307411; PJK).

References

- Barnes, J. R., Collier Cameron, A., Donati, J.-F., et al. 2005, in ESA Special Publication, Vol. 560, 13th Cambridge Workshop on Cool Stars, Stellar Systems and the Sun, ed. F. Favata, G. A. J. Hussain, & B. Battrick, 95
- Benomar, O., Bazot, M., Nielsen, M. B., et al. 2018, *Science*, 361, 1231
- Brandenburg, A. & Giampapa, M. S. 2018, *ApJ*, 855, L22
- Chan, K. L. 2001, *The Astrophysical Journal*, 548, 1102
- Donati, J.-F. & Collier Cameron, A. 1997, *Month. Not. Roy. Astr. Soc.*, 291, 1
- Featherstone, N. A. & Miesch, M. S. 2015, *The Astrophysical Journal*, 804, 67
- Gastine, T., Yadav, R. K., Morin, J., Reiners, A., & Wicht, J. 2014, *Month. Not. Roy. Astr. Soc.*, 438, L76
- Hathaway, D. H., Upton, L., & Colegrove, O. 2013, *Science*, 342, 1217
- Hupfer, C., Käpylä, P. J., & Stix, M. 2006, *Astronomy & Astrophysics*, 459, 935
- Käpylä, P. J. 2018, *Astronomy & Astrophysics* (submitted), arXiv:1812.07916
- Käpylä, P. J. 2019, *Astronomy & Astrophysics* (in press), arXiv:1712.08045
- Käpylä, P. J., Korpi, M. J., & Tuominen, I. 2004, *Astronomy & Astrophysics*, 422, 793
- Käpylä, P. J., Mantere, M. J., & Brandenburg, A. 2011, *Astronomische Nachrichten*, 332, 883
- Kövári, Z., Oláh, K., Kriskovics, L., et al. 2017, *Astronomische Nachrichten*, 338, 903
- Kippenhahn, R. 1963, *The Astrophysical Journal*, 137, 664
- Kitchatinov, L. L. & Oleskoy, S. V. 2011, *Month. Not. Roy. Astr. Soc.*, 411, 1059
- Kitchatinov, L. L., Pipin, V. V., & Rüdiger, G. 1994, *Astronomische Nachrichten*, 315, 157
- Kitchatinov, L. L. & Rüdiger, G. 1999, *Astronomy & Astrophysics*, 344, 911
- Kitchatinov, L. L. & Rüdiger, G. 2004, *Astronomische Nachrichten*, 325, 496
- Küker, M. & Rüdiger, G. 2018, *Astronomische Nachrichten*, 339, 447
- Küker, M., Rüdiger, G., & Kitchatinov, L. L. 2011, *Astronomy & Astrophysics*, 530, A48
- Künstler, A., Carroll, T. A., & Strassmeier, K. G. 2015, *Astronomy & Astrophysics*, 578, A101
- Metcalfe, T. S., Egeland, R., & van Saders, J. 2016, *ApJ*, 826, L2
- Ossendrijver, M. 2003, *A&A Rev.*, 11, 287
- Reinhold, T. & Arlt, R. 2015, *Astronomy & Astrophysics*, 576, A15
- Reinhold, T., Reiners, A., & Basri, G. 2013, *Astronomy & Astrophysics*, 560, A4
- Rüdiger, G. 1989, *Differential rotation and stellar convection. Sun and the solar stars* (Berlin: Akademie Verlag, 1989)
- Rüdiger, G., Egorov, P., & Ziegler, U. 2005, *Astronomische Nachrichten*, 326, 315
- Rüdiger, G., Küker, M., & Schnerr, R. S. 2012, *Astronomy & Astrophysics*, 546, A23
- Solanki, S. K. 2003, *A&A Rev.*, 11, 153
- Strassmeier, K. G. 2009, *A&A Rev.*, 17, 251
- Warnecke, J., Käpylä, P. J., Mantere, M. J., & Brandenburg, A. 2013, *The Astrophysical Journal*, 778, 141
- Wöhl, H., Brajša, R., Hanslmeier, A., & Gissot, S. F. 2010, *Astronomy & Astrophysics*, 520, A29
- Ziegler, U. 2002, *Astronomy & Astrophysics*, 386, 331

Q_{xz}



$Q_{xz}/\sin \theta$

